Separation and Purification Technology 168 (2016) 168–176

Contents lists available at ScienceDirect

Separation and Purification Technology

journal homepage: www.elsevier.com/locate/seppur

A sustainable affinity partitioning process to recover papain from *Carica papaya* latex using alginate as macro-ligand

Maria Victoria Rocha [a], Melisa Di Giacomo [a], Sofía Beltramino [a], Watson Loh [b], Diana Romanini [a], Bibiana Beatriz Nerli [a,*]

[a] Instituto de Procesos Biotecnológicos y Químicos (IPROBYQ), Consejo Nacional de Investigaciones Científicas y Técnicas (CONICET), Facultad de Ciencias Bioquímicas y Farmacéuticas, Universidad Nacional de Rosario, Suipacha 570, S2002LRK Rosario, Argentina
[b] Instituto de Química, UNICAMP, Rua José de Castro, s/n – Cidade Universitária, Campinas – Caixa Postal 6154, Campinas, SP CEP 13083-970, Brazil

ARTICLE INFO

Article history:
Received 5 March 2016
Received in revised form 12 May 2016
Accepted 26 May 2016
Available online 27 May 2016

Keywords:
Affinity partitioning
Aqueous two-phase systems
Papain
Alginate

ABSTRACT

The role of the natural biodegradable polymer alginate (ALG) as affinity macro-ligand for papain (PAP) was evaluated in order to design a new sustainable two-phase affinity strategy for recovering this enzyme from *Carica papaya* latex.

In presence of PAP, decreased values of intrinsic viscosity and hydrodynamic radius of ALG were observed. These results suggested a neutralizing effect of PAP on the polymer negative charges which caused a decrease of intra-chain repulsion forces in ALG molecules and a consequent shrinkage of the polymer size. Calorimetric measurements demonstrated a cooperative interaction between PAP and ALG which was enthalpy-entropically driven.

When partitioned *C. papaya* latex into aqueous two-phase systems (ATPSs) formed by polyethylene glycol (PEG) of MW 8000 and the biodegradable salt sodium citrate pH 5.20, only 20% of PAP was recovered at the PEG-enriched phase with a purification factor (PF) of 2.48. The addition of ALG 0.1% (w/w) into the system doubled the PAP partition coefficient ($K_{p,\ PAP}$), showing the ability of this polymer to enhance the enzyme recovery at the PEG-enriched phase and therefore, increasing the extraction efficiency. The subsequent addition of calcium chloride at a final concentration of 80 mM allowed the precipitation of the target enzyme and the recovering of PEG phase for recycling. The overall process showed a PAP recovery of 72% and a PF of 2.41. The proposed strategy not only conserved all the advantages of the reported extractions with PEG/ammonium sulfate (or phosphate) ATPSs, i.e., low cost, scalability and integration of the clarification and extraction steps, but also allowed overcoming their main drawbacks, i.e., the separation of the target molecule from the phase-polymer and the environmental impact caused by the disposal of these salts.

1. Introduction

Proteases play an important role in industrial processes due to their ability of transforming materials, i.e. protein structure and functionality, with high rate at sustainable conditions. Most commercialized proteases are those coming from microbial sources. However, some plant cysteine proteases such as papain (PAP) are still preferred and currently used for certain industrial applications due to its specificity and stability properties [1,2]. Papain (EC3.4.22.2) is a cysteine endopeptidase present in the latex of papaya fruit which has been extensively used in food industries as meat tenderizer, for stabilizing and chill-proofing beer and in baking processes. Besides, it has been applied in textile and pharmaceutical industries, and also for effluent treatments [3].

Currently, PAP is recovered from its natural source by a given combination of unit operations such as clarification, precipitation with salts, extraction with solvents, chelating or reducing agents, chromatographic techniques [4], filtration and spray-drying. Environmental impact, cost of resins, time-consuming processes, occupational allergies and unstable yielding products are the main disadvantages reported for the above mentioned downstream processes [2]. Alternative methods tending to avoid or minimize these difficulties have been developed.

Extraction with aqueous two-phase systems (ATPSs) is a methodology that integrates the clarification, concentration and purification of the target product in one unit operation. It exhibits many advantages including low cost, easy scalability and mild

* Corresponding author.
E-mail address: bnerli@fbioyf.unr.edu.ar (B.B. Nerli).

http://dx.doi.org/10.1016/j.seppur.2016.05.025
1383-5866/

conditions to preserve biological molecules. Besides, it does not require sophisticated equipment [5] thus becoming an attractive strategy for industrial purposes. Different polymer/salt ATPSs such as polyethylene glycol (PEG)/phosphate [6] and PEG/ammonium sulfate [2,4] have been earlier reported for the extraction of PAP from papaya latex. Although the high PAP recoveries obtained with these systems, close to 90%, they presented two main drawbacks: the difficulty to isolate the extracted molecule from the polymer phase by back extraction and the use of high salt concentrations which becomes critical at process-scale and requires of disposal and corrosion considerations. Particularly, the use of ammonium sulfate and phosphates for any manufacturing process is discouraged since its discharge into water bodies can result in the promotion of algal growth and subsequent creation of anaerobic conditions. The treatment and disposal of wastes, required to minimize their impact, increase the downstream processing costs and consequently decrease their economic viability. In this context, the design of extracting protocols with ATPSs formed by biodegradable and/or recyclable components, would be desirable [7–9].

Affinity partitioning using smart macro-ligands is a powerful method used for separation of biomolecules [10,11] which integrates two-phase partitioning and affinity precipitation. The affinity macro-ligand is incorporated into the PEG/salt ATPS with the aim of directing the partitioning of the target molecule to the polymer-rich phase. Later, the precipitation of the ligand-biomolecule complex with an appropriate stimulus – pH, temperature, presence of certain ions – allows recovering both, the target molecule (PEG-free) and the phase polymer (PEG) which can be reused in a new extraction cycle. Affinity ligands are considered suitable for this purpose when they partition unevenly to the PEG phase, bind selectively/reversibly to the target biomolecule and can be precipitated/re-dissolved by changing medium conditions. Chitosan, Eudragit S-100 and alginate, among other polymers, fulfill these requisites [12], thus being widely used in these strategies [13]. Particularly alginate, a polysaccharide of marine origin, consisting of mannuronic (M-block) and guluronic (G-block) acid units has demonstrated to be appropriate to recover Bacillus acidopullulyticus pullulanase from a crude enzyme preparation [12], beta-amylase from sweet potato [14] and phospholipase D from peanuts [15]. Several reports have addressed on the ability of calcium alginate beads of immobilizing and stabilizing papain [16,17]. However, as far as we know, soluble sodium alginate (ALG) has not been used as bio-ligand for this protease in affinity strategies.

The aim of this work was to evaluate the suitability of ALG to be used as a macro-ligand for PAP in order to develop a new affinity partitioning process capable of recovering this protease from *Carica papaya* latex. The use of ALG in a PEG/sodium citrate (biodegradable salt) ATPS is expected to enhance the extraction of papain to the polymer-rich phase and allow its subsequent recovery by precipitation. The resulting strategy will allow overcoming the main disadvantages reported for the extraction with PEG/ammonium sulfate (or phosphate) ATPS such as the separation of the target molecule from the phase-polymer and the environment impact associated to the disposal of these salts.

2. Materials and methods

2.1. Chemicals and raw materials

Polyethylene glycols of different molecular weights (PEG600, PEG1000, PEG2000, PEG4600 and PEG8000), alpha-*N*-benzoyl-DL-arginine-*p*-nitroanilide (BAPNA) and sodium alginate (ALG) of low viscosity, composed primarily of mannuronic acid residues, were purchased from SIGMA-Aldrich (USA). All other chemicals were of analytical grade. Commercial papain (PAP_{com}) from *C. papaya* latex was also purchased from Sigma Chem. Co. Stock solutions (4000 μM) of this protease in 100 mM sodium phosphate buffer pH 6.00 were gravimetrically prepared and kept at −18 °C until use. Stock solutions of ALG 2% (w/w) and PEGs 30% (w/w) were prepared by dissolving appropriate quantities of polymer in distilled water.

Fresh latex was collected from locally grown *C. papaya* trees. After washing the fruits with distilled water, several vertical incisions were made along the surface with a knife to a depth of 2–3 mm. The exuded latex was collected into a glass beaker set on ice. After collection, the latex was fractionated and stored at −18 °C. Thawed latex was dissolved in phosphate buffer pH 6.0 and the obtained suspension was referred to as "crude papain extract" (CPE). Its content of papain (PAP_{latex}), reducing sugars (RS) and total proteins (TP) was determined as described below.

2.2. Procedures

2.2.1. Partitioning measurements

2.2.1.1. Preparation of aqueous two-phase systems. Aqueous two-phase systems (ATPSs) with a final mass of 2 g were prepared by weighing appropriate quantities of stock solutions of PEGs of different molecular weight 30% (w/w), sodium citrate (NaCit) 25% (w/w) pH 5.20 and distilled water. The sodium citrate stock solution was prepared from a citric acid solution whose pH was adjusted to 5.20 by the addition of appropriate quantities of sodium hydroxide. At the mentioned pH, acid and base conjugate forms of citric acid coexist ($pKa_{2\ citric\ acid} = 4.76$) thus resulting in a mixture with buffer capability.

Table 1 shows the tie line length (TLL), the total and the phase compositions of the selected systems. ATPSs containing ALG as affinity macro-ligand were prepared by including appropriate amounts of ALG stock solution in the above mentioned systems to reach the desired ALG total final concentration of 0.1% (w/w). In this case, water content was reduced appropriately to keep the PEG and NaCit total concentrations unaltered.

2.2.1.2. Determination of partition coefficients. Partitioning behavior of papain (PAP_{com} and PAP_{latex}), sodium alginate (ALG), reducing sugars (RS) and total proteins (TP) in the assayed ATPSs were evaluated through their partitioning coefficients ($K_{p,\ PAPcom}$; $K_{p,\ PAPlatex}$; $K_{p,\ ALG}$; $K_{p,\ RS}$; $K_{p,\ TP}$) defined as:

$$K_{p,M} = \frac{[M]_{top}}{[M]_{bottom}} \quad (1)$$

where $[M]_{top}$ and $[M]_{bottom}$ represent the concentration of the partitioned molecule (M): PAP_{com}, PAP_{latex}, ALG, RS and TP at both top and bottom phases after reaching the equilibrium condition.

The procedure consisted of dissolving a given amount of either stock solutions (ALG, PAP_{com}) or crude papain extract (CPE) into the

Table 1
Total, bottom and top compositions of ATPSs formed by PEGs of different molecular weights and NaCit pH 5.20.

PEG molecular weight	TLL % (w/w)	Total composition % (w/w)		Bottom composition % (w/w)		Top composition % (w/w)	
		PEG	NaCit	PEG	NaCit	PEG	NaCit
600	48.37	21.00	16.20	0.77	27.89	42.65	3.69
1000	26.42	15.92	13.97	5.10	19.01	28.87	7.47
2000	41.44	13.75	14.40	0.13	21.59	36.78	2.24
4600	24.98	11.70	9.65	0.88	14.18	23.92	4.53
8000	24.42	11.69	9.52	1.44	13.52	24.19	4.63

TLL, tie line length.

ATPS. The aliquots of loaded material did not exceed the 10% of total system weight to prevent changes in binodal compositions. After mixing by inversion for 15 min and leaving it to settle for at least 90 min in a 20 °C bath, the system was centrifuged 5 min at low speed (2000 rpm) for phase separation. Phase volumes were measured and appropriate amounts of each phase were removed to determine the macromolecule concentration [M] in each phase.

When partitioning CPE, the purification factor (PF) and the recovery percentage (R%) of PAP at a given phase (top/bottom) were also calculated as follows:

$$PF_{top/bottom} = \frac{Act_{top/bottom}/[TP]_{top/bottom}}{Act_{CPE}/[TP]_{CPE}} \quad (2)$$

$$R_{top/bottom}\% = \frac{Act_{top/bottom}V_{top/bottom}}{Act_{CPE}V_{CPE}}100 \quad (3)$$

where Act is the enzyme activity; [TP], the concentration of total proteins; $V_{top/bottom}$, the volume of phase (top/bottom) and V_{CPE}, the volume of CPE loaded into the ATPS.

All partition experiments were performed in triplicate. The mean K_p values and their estimated standard deviations were informed in each case. Mass balance (%) was also calculated for each molecule after partitioning.

2.2.1.3. Determination of aqueous two-phase diagrams. Two-phase diagrams of PEG8000/NaCit ATPS were determined in the absence and presence of ALG 0.1% (w/w). The binodal curves were obtained, as described in previous works [18], by the turbidimetric titration of a PEG8000 stock solution 30% (w/w) with small aliquots of NaCit stock solution 25% (w/w) pH 5.20 until the system turned into a turbid solution (cloud point). The masses of the starting and added solutions, measured on an analytical balance, were used to calculate the composition of the mixture for each point on the binodal curve. The temperature of the system was kept constant at 293 K and controlled within ±0.1 K. Binodal data were fitted with different expressions reported for these systems, the best results being obtained with the Mistry equation [19]. Phase diagrams in presence of ALG were obtained similarly by using PEG and NaCit stock solutions containing ALG 0.1% (w/w).

The nodes and tie lines were determined by the method described by Merchuk et al. [20] based on the application of the lever-arm rule on binodal diagram. The knowledge of both, the function describing the binodal curve (Mistry equation) and the top/bottom mass ratio of each system were required. For the latter, three systems of different total compositions were prepared into graduate tubes, stirred thoroughly and left to reach phase separation for 24 h. Top/bottom mass ratio was calculated from volume and density measurements.

2.2.2. Analytical determinations

Papain (PAP_{com}, PAP_{latex}) content was determined by measuring its amidase activity against the chromogenic reagent BAPNA [21]. The substrate was used at a final concentration of 1 mM in 50 mM TRIS buffer pH 8.20 with 12 mM cysteine. The reaction was followed by measuring the absorbance of the released reaction product, p-nitroaniline, at 400 nm for 5 min.

The assay was performed at 25 °C in a thermostatized spectrophotometer cell. The enzyme activity was calculated from the initial linear portion of absorbance vs. time curve.

The total protein content (TP) in the CPE and in each phase was estimated by the Warburg and Christian method [22] using the specific software of spectrophotometer JASCO V-550 UV–vis.

Reducing sugars (RS) in the CPE and in each phase were also determined by the dinitrosalycilic acid (DNS) colorimetric method [23]. Glucose (40 mM) was used as the analytical standard at a concentration range of 0.3–1.5 mM in 50 mM NaCit buffer pH 5.20 to obtain calibration curves for top and bottom phases.

Alginate concentration in both phases was estimated by the phenol sulphuric acid method [24].

2.2.3. Measurements to evaluate the alginate as an affinity macroligand

2.2.3.1. Viscometry. Alginate solutions with final concentrations (C_{ALG}) between 0.02 and 0.10% (w/v) were prepared by diluting ALG stock solution 2% (w/w) in buffer NaCit 25% (w/w) pH 5.20. The relative viscosity (η_R) of each solution was calculated as the ratio between the drainage times of the ALG solutions and the buffer. The intrinsic viscosity, [η], and the Huggins constant, k_H, parameters associated with the polymer conformation, were determined by applying the Huggins equation [25]:

$$\frac{\eta_R - 1}{C_{ALG}} = [\eta] + k_H[\eta]^2 C_{ALG} \quad (4)$$

which shows a linear dependence of reduced viscosity, $(\eta_R - 1)/C_{ALG}$, with the C_{ALG} for dilute solutions. The [η] and k_H values were obtained from the intercept and the slope of the $(\eta_R - 1)/C_{ALG}$ vs. C_{ALG} plot in the absence and presence of PAP 0.4% (w/w). Viscosity measurements were performed by using an Ubbelohde-type capillary automated microviscometer immersed in a thermostatized water bath at (25 ± 0.05) °C [26].

2.2.3.2. Dynamic light scattering (DLS). Solutions of ALG 0.1% (w/w), PAP_{com} (5 μM) and ALG + PAP were clarified by filtration and centrifugation procedures in order to make them completely transparent, condition which was verified by turbidity measurements. DLS measurements were performed on a Nano Particle Analyzer SZ-100 (Horiba). The light source was a He–Ne laser operating at a wavelength of 633 nm with 90° scattering angle. Measurements corresponding to the ALG, PAP and ALG + PAP solutions were performed at least three times each. The apparent hydrodynamic radius (R_h) of particles present in each system was calculated by using the Stokes–Einstein relationship.

2.2.3.3. Isothermal titration calorimetry (ITC). Measurements were performed at 20 °C in an isothermal titration calorimeter (VP-ITC, MicroCal Inc., USA). Aliquots from 3 to 15 μL of PAP_{com} solution (0.20 mM) were injected sequentially into a 1.436 mL titration cell initially containing either buffer solution (50 mM NaCit pH 5.20) or ALG solution (0.50% (w/w)) in NaCit buffer. Each injection lasted between 6 and 30 s and there was an interval of 600 s between successive injections. Corrected enthalpy changes were calculated by subtracting the enthalpy change when PAP was titrated into buffer solution from that obtained when PAP was titrated into ALG solution. Enthalpy change associated to the ALG dilution (when buffer was titrated into ALG solution) was also subtracted. Titrations were carried out in duplicate and the results were reported as the mean. The resulting data, expressed as the change in enthalpy per mole of PAP (23,400 Da) vs. the molar ratio n_{PAP}/n_{ALG}, were fitted to a sequential binding model consisting of two stages. The affinity constant (K), the enthalpy and entropy changes (ΔH°, ΔS°), associated to the binding, were estimated using the MicroCal ORIGIN 7.0 software supplied by the instrument.

2.2.4. Affinity partitioning protocol

Aqueous two-phase systems formed by PEG8000 11.69% (w/w), NaCit 9.52% (w/w) and ALG 0.1% (w/w) were prepared according to the procedure of Section 2.2.1. The two-phase affinity strategy designed consisted of three subsequent steps.

Step 1: The CPE (150 μL) was loaded into an ATPS of 2 g of total mass. After mixing by inversion and leaving it to settle for

90 min at 20 °C, the system was centrifuged (5 min at 2000 rpm) for phase separation. Phase volumes were measured and most of top phase, (containing PAP) was recovered with a pipette to perform the following step.

Step 2: Top phase (1.25 mL) was mixed with 4.75 mL of an aqueous ALG solution 1.4% (w/w). This allowed reducing the ionic strength and reaching a final ALG concentration close to 1% (w/w), both conditions being required to form the complex ALG-PAP (this is based on experimental data obtained in our laboratory, not shown in this work). Then, the total ALG (free and bound to PAP) was precipitated by dropping slowly a solution of $CaCl_2$ (1 M) until a final $CaCl_2$ concentration of 80 mM. After 30 min of incubating at 8 °C, the precipitate (PP_{step2}) and the supernatant (SN_{step2}) were separated by centrifugation at 4000*g* for 10 min at 20 °C.

Step 3: Finally, the PP_{step2} was dissolved by incubation with a mixture of 1.75 mL de NaCit 25% (w/w) and 0.250 mL of NaCl 4 M for 2.5 h at 8 °C. The final volume of the obtained solution (SL_{step3}) was measured.

Enzyme activity and total protein content were determined in each step to calculate the PF and R% extraction indicators.

3. Results and discussion

3.1. Partitioning experiences

Previous reports demonstrated the good performances of different ATPSs at recovering papain from *C. papaya* latex [6,15]. However, the phase forming salts of these systems, ammonium sulfate and sodium phosphate, are known to cause soil/water acidification and eutrophication when they are released to the environment excessively. In an attempt to reduce this impact, we evaluated the extraction ability of systems formed by PEGs of different molecular weights and a biodegradable salt (NaCit). The distribution behavior of PAP after partitioning the crude extract in these systems is shown in Fig. 1.

It is appreciated that PAP_{latex} was displaced to the bottom phase in all the systems assayed with $K_{p,\ PAP}$ values between 0.5 and 0.8 (Fig. 1A). This pattern is quite similar to that obtained for commercial PAP in a previous work [7]. The decrease of $K_{p,\ PAP}$ with PEG molecular weight (from PEG600 to PEG4600) could be explained by the prevalent top-phase exclusion effect caused by the increasing size of the polymer. A slight increase of $K_{p,PAP}$ was appreciated in systems formed by PEG8000, probably due to a major role of the interactions of PAP with the rest of the components of the mixture.

The uneven distribution of PAP led to different recoveries, R%, at top and bottom phases, the highest values being observed for the salt-enriched bottom phase (Fig. 1A). Mass balances close to 100% were obtained for PAP in all cases, indicating that no significant amounts of this protein were lost at ATPSs interfaces. However, variable quantities of insoluble matter (cell debris and particulate components of the latex clot) were detected between the phases after reaching the equilibrium. This feature indicated that sample clarification was taking place simultaneously with the partitioning phenomenon.

When analyzed the PF values (Fig. 1B), the best purification performance was observed at the top phase. Particularly, a PF of 2.5 was achieved in the top phase of PEG8000/NaCit systems. On the basis of these results, two alternatives were evaluated. Selecting the bottom phase and recovering most of the PAP without an appreciable purification grade or selecting the top phase reaching better purification performances but losing significant amounts of the target protein. Our challenge was to achieve both, a significant recovery and a good purification factor in the selected phase.

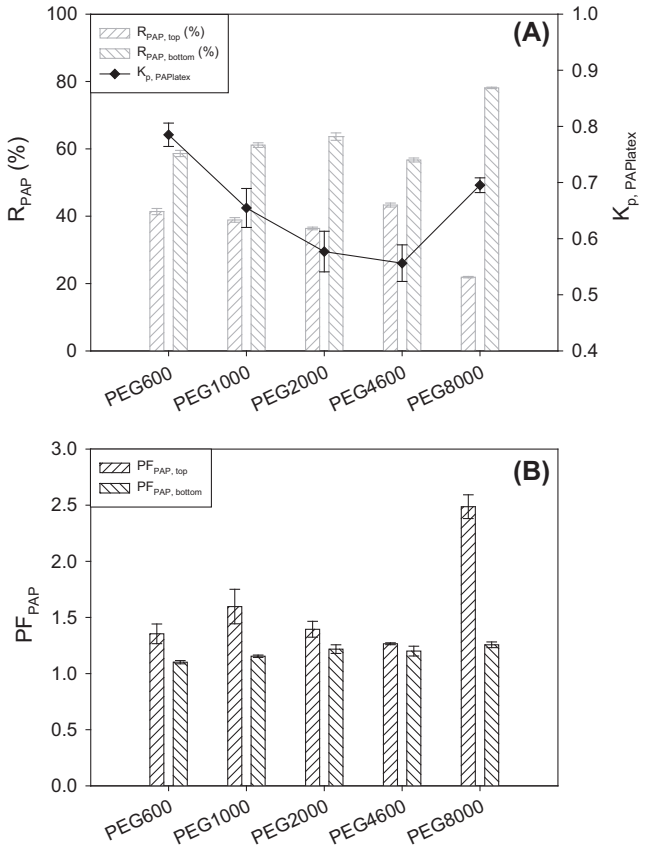

Fig. 1. Partitioning coefficients, recoveries and purification factors corresponding to the extraction of PAP from *C. papaya* latex with ATPSs formed by PEGs of different molecular weight and NaCit pH 5.20. Compositions of ATPSs are given in Table 1. Temperature 20 °C.

It is worth of consideration that main contaminants of commercial PAP are other proteins contained in latex such as lysozyme, lipase, trypsin-inhibitor like protein, chitinase [27]. Their presence in the final product adds potentially undesirable enzyme activities or prevents the optimal functionality of the target protein. This fact was considered when optimized the PF value since its calculation took into account the total protein content of each phase. However, contamination with small molecules such as fats, sugars, and vitamins, also present in the CPE, was not considered. These residual impurities could potentially impact the protein stability and affect its quality [28]. Reducing sugars are known to form glycation products with proteins via the Maillard reaction during the storage stage, thus changing their stability/activity characteristics. Particularly, PAP was reported to lose the 70% of its initial activity after incubating with glucose 300 mg/dL for two weeks [29,30]. Because of this, partitioning behavior of reducing sugars (RS), present in latex, was also studied.

Fig. 2 shows that the partitioning of RSs was displaced to the bottom phase in all cases with $K_{p,\ RS}$ values lower than 0.1. The separation coefficient (β), calculated as the ratio $K_{p,PAP}/K_{p,\ RS}$, adopted high values (>7.5) in all the systems. ATPSs formed by PEG2000 and PEG4600 demonstrated to have the best capability of separating PAP from RSs, however, in these systems both the protein and the reducing sugars are mostly recovered at the bottom phase. Due to the low recoveries (20–40%) observed for PAP at the top phase, the inclusion of an affinity ligand, able to drive selectively PAP partitioning to the top phase, seemed to be an appropriate tool to enhance protein recovery.

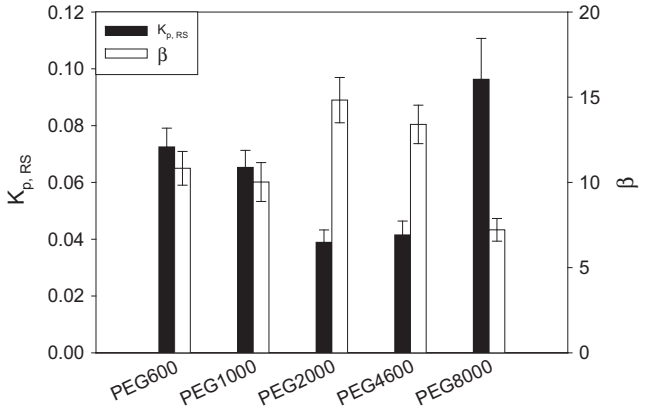

Fig. 2. Partitioning behavior of reducing sugars (RS) of *C. papaya* latex in ATPSs formed by PEGs of different molecular weight and NaCit pH 5.20. Separation factor (β) was calculated as the ratio $K_{p, PAP}/K_{p, RS}$. Compositions of ATPSs are given in Table 1. Temperature 20 °C.

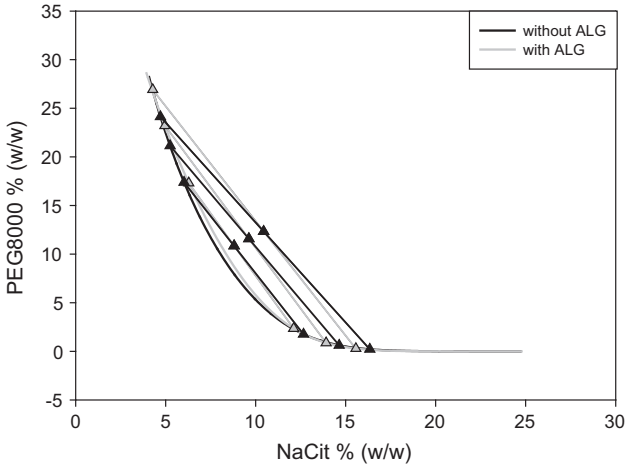

Fig. 4. Effect of presence of ALG on the binodal curve and nodes corresponding to the phase diagram of PEG8000/NaCit pH 5.20. Temperature 20 °C.

The use of alginate (ALG) as a macro-ligand in two-phase affinity extractions has been reported for other proteins [14,31]. To evaluate the effect of this polymer on the partitioning behavior of PAP, only those systems formed by PEG2000, PEG4600 and PEG8000 were selected due to their higher values of either β or PF. The results, depicted in Fig. 3, indicated that ALG partitioning equilibrium was displaced to the PEG enriched-phase in all the systems. Similar trend was observed for chitosan, carrageenan and even for alginate in ATPSs of PEGs and other salts different from NaCit [15,32]. This uneven partition is a requisite that any ligand must fulfill to be used in a two-phase affinity extraction [33].

Fig. 3 also shows that PAP partitioning was driven to the top phase when ALG was included in the ATPSs. Although the drastic enhancements of $K_{p, PAP}$ values observed in all the systems, only that formed by PEG8000 showed to displace the PAP to the top phase significantly, thus achieving a $K_{p\ PAP}$ value of 2.4. The driving-effect exerted by ALG on PAP partitioning could be caused either by changes in PEG and NaCit equilibrium concentrations (derived from the inclusion of ALG in the ATPS) or by a selective interaction between ALG and PAP molecules, the latter being a condition necessary to develop a two-phase affinity extraction. To explore the effect of ALG on the concentration of phase forming components, the binodal diagrams in absence and presence of ALG were determined (Fig. 4). No significant changes in binodal curve and equilibrium compositions were observed. In a previous work [7], we analyzed the effect of tie line length on $K_{p, PAP}$ and we observed that changes in system compositions, higher than those caused by the presence of ALG, did not change PAP partitioning significantly. This suggests that the strong driving effect of ALG on PAP partitioning to the top phase would not be caused by alterations in system composition. Therefore, the second alternative above mentioned, i.e. selective interaction ALG-PAP, was evaluated.

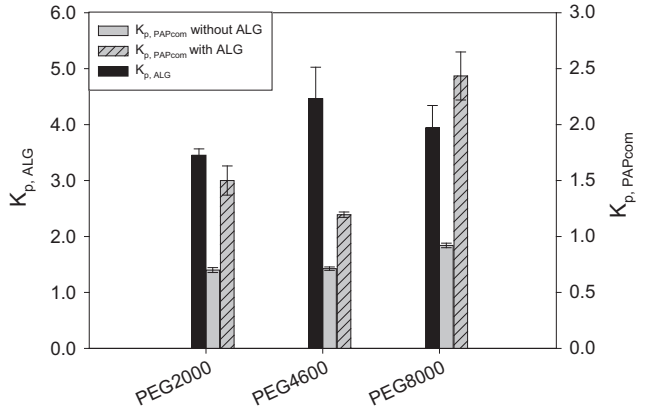

Fig. 3. Effect of ALG on the partitioning behavior of PAP. Final ALG concentration in each ATPSs was 0.1% (w/w). Compositions of ATPSs are given in Table 1. Temperature 20 °C.

3.2. Evaluation of ALG as an affinity macro-ligand for PAP

Alginate is a linear polymer of (1 → 4)-β-D-mannuronopyranosyl and (1 → 4)-α-L-guluronopyranosyl units. The dissociation constants of its acid residues (3.38–3.65) make this polymer acquire increasing negative charge at pHs higher than 4.00, thus becoming an anionic polyelectrolyte. Considering PAP as a globular protein with a pI close to 9.00, the interaction between PAP and ALG, both carrying opposite net charges at working conditions (pH 5.20), would be expectable. A rational approach tending to probe this intuitive presumption is required to support scientifically the experimental observations. For this purpose, several complementary techniques such as viscometry, dynamic light scattering and isothermal titration calorimetry were carried out.

Viscometry is a sensitive and useful tool for describing the behavior of flexible chain polymers in solution [34]. Reduced viscosities, $(\eta_R - 1)/C_{ALG}$, determined for ALG solutions in absence and presence of PAP are depicted in Fig. 5. The intrinsic viscosity ([η]) and the Huggins constant (k_H) in each case are also shown within the figure.

The plot obtained for ALG in absence of PAP exhibited a linear pattern where the reduced viscosity decreased with the polymer concentration. This behavior, typical of polyelectrolytes, was reported to derive from the intra-chain electrostatic forces between the charges of chain backbone which leads to an increase of reduced viscosity upon dilution [35].

The value of intrinsic viscosity obtained (6.07 dL/g) was far higher than the value corresponding to a random coil polymer (3.04 dL/g) of the same molecular weight (66,000 Da), calculated according to the Mark-Houwink equation [36]. This finding is in concordance with a more extended and stiff conformation for the ALG molecule. In presence of PAP, the dependence of reduced viscosity with ALG concentration showed an inverted trend. A linear plot with positive slope, typical of random coil polymers, with an intrinsic viscosity value of 3.45 dL/g was observed. This behavior

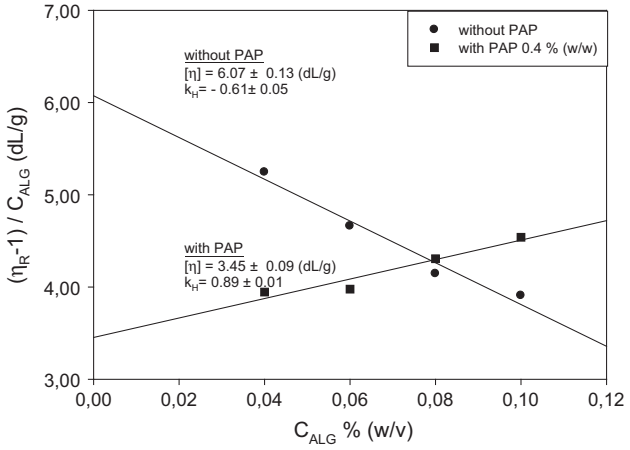

Fig. 5. Differences in viscometry behavior of ALG and ALG + PAP solutions. Temperature 25 °C.

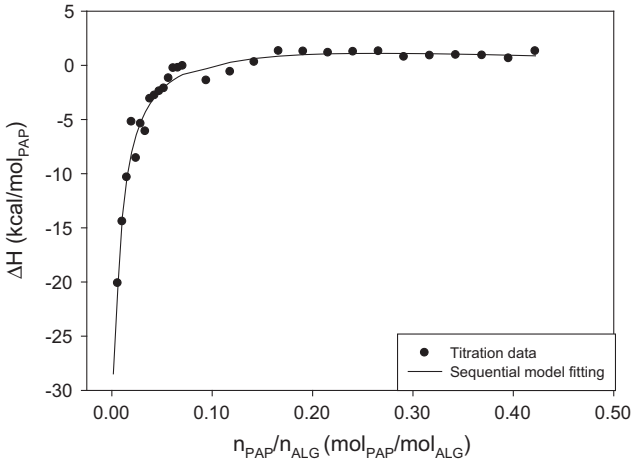

Fig. 6. Isothermal titration calorimetry of ALG solution (0.092 mM) contained in a reaction cell with PAP (0.200 mM) in 50 mM NaCit buffer pH 5.20. Temperature 20 °C.

could be explained by a neutralizing effect of PAP on polymer negative charges which causes a decrease of intra-chain repulsion forces in the ALG molecules and a consequent shrinkage of the polymer size. Similar behavior was reported for ALG in presence of cationic surfactants [37].

Dynamic light scattering measurements were carried out to get information about the size of ALG and PAP individually and after mixing them. It is worth of noticing that biopolymer concentrations used in DLS measurements were very low to avoid turbidity derived from the aggregation phenomenon. The results of DLS are shown in Table 2. As observed, PAP hydrodynamic radius (R_h) was in the range 3–4 nm in concordance with the value of 4.2 nm reported by other authors [38] for the native conformation. For ALG solutions, a larger R_h was observed due to the stiff chain conformation of ALG polymer, above discussed. When compared with data of R_h corresponding to ALG in literature, diverse values in the range 138–600 nm were found, depending on both the medium conditions (pH, ionic strength, etc.) and the polymer molecular weight [39,40]. The ALG + PAP mixture presented a mean size lower than that observed for the ALG alone. A decrease in the repulsion among negative charges in ALG, caused by its interaction with PAP, would be taking place thus decreasing the molecule stiffness and therefore, its size. This agrees with the trend observed in viscometry.

On the basis of the preceding results, the interaction and complex formation between PAP and ALG were also assessed by microcalorimetric techniques. Fig. 6 shows the curve for the isothermal calorimetric titration of 200 μM PAP into 92 μM ALG in buffer NaCit 50 mM pH 5.20.

As observed, the resulting data were fitted satisfactorily to a sequential binding model of two stages. The affinity constant of each step (K_1, K_2), the molar enthalpy changes for the binding ($\Delta H_1°$, $\Delta H_2°$) and the molar entropy changes ($\Delta S_1°$, $\Delta S_2°$) were estimated from the fitted curve and summarized in Table 3.

Table 2
Mean hydrodynamic radius (R_h) of biopolymer solutions containing PAP, ALG and a PAP + ALG mixture, obtained from DLS measurements.

Biopolymer solution	R_h (nm)
PAP	3.49 ± 0.78
ALG	193.48 ± 36.18
ALG + PAP	137.20 ± 30.71

$C_{ALG} = C_{PAP}$ = 0.01% (w/w).

The affinity value for the first binding stage adopted a moderate value (10^4 M^{-1}) but it increased drastically when bound the second PAP molecule (10^6 M^{-1}). This evidenced the presence of a positive cooperative effect in the interaction between both biopolymers. Analysis of thermodynamic parameters indicated that the binding of the first PAP molecule to ALG was enthalpically driven ($\Delta H_1° < 0$, $\Delta S_1° < 0$), thus suggesting the presence of electrostatic forces in the interaction. The opposite behavior ($\Delta H_2° > 0$, $\Delta S_2° > 0$) observed for the second step (entropically driven), suggested the participation of a "hydrophobic effect" component in the binding [41]. This combination of enthalpic and entropic steps allow us to postulate that the negatively charged carboxyl groups of ALG would be interacting with the opposite ones in PAP (protonated lysyl and histidyl groups) at initial binding stages. As a consequence, the hydrophobic chain backbone of ALG would get more exposed and then, would become capable of interacting, in a second stage, with hydrophobic pockets present in PAP molecule.

It is important to notice that the stoichiometry of ALG-PAP complex was not achieved due to the lack of titration data at the initial region of the curve caused by sensibility issues. However, a visual inspection of Fig. 6, lead us to predict a saturation fractional ratio (n_{PAP}/n_{ALG}) which indicates that one molecule of PAP binds several ALG molecules. This agrees with the behavior observed for other protein-polysaccharide interactions [42].

3.3. Two-phase affinity partitioning

According to the partitioning experiences above discussed, the system formed by PEG8000 and NaCit seemed to be the most appropriate to develop a strategy of affinity extraction. The uneven partitioning of ALG to the PEG-enriched phase, its ability of interacting tightly with PAP, its capability of being precipitated reversibly with calcium ions in addition to its excellent properties (i.e., biodegradability, non-toxicity, non-immunogenicity and biocompatibility) make this polymer become an excellent candidate to be used as an affinity macro-ligand. Fig. 7 shows a schematic representation of the strategy carried out for the extraction of PAP_{latex}. All the necessary conditions (ionic strength, calcium chloride concentration, aliquots, etc.) required to precipitate and dissolve ALG complexes are detailed in Section 2.2.4. They were determined in our laboratory by optimizing the starting information reported [11,15]. Fig. 7 also shows an additional last step to re-precipitate ALG for recycling and recover PAP free of ALG. To carried out this

Table 3
Binding and thermodynamic parameters associated to a two-step sequential model for the interaction between PAP and ALG, obtained from ITC measurements.

First sequential step			Second sequential step		
K_1 (M^{-1})	$\Delta H_1°$ (cal/mole)	$\Delta S_1°$ (cal/K mole)	K_2 (M^{-1})	$\Delta H_2°$ (cal/mole)	$\Delta S_2°$ (cal/K mole)
$1.27 \cdot 10^4 \pm 7.00 \cdot 10^3$	$-5.88 \cdot 10^4 \pm 1.73 \cdot 10^4$	-178 ± 17	$1.23 \cdot 10^6 \pm 3.70 \cdot 10^5$	$8.18 \cdot 10^4 \pm 1.70 \cdot 10^4$	302 ± 25

Thermodynamic parameters are expressed per mole of PAP.

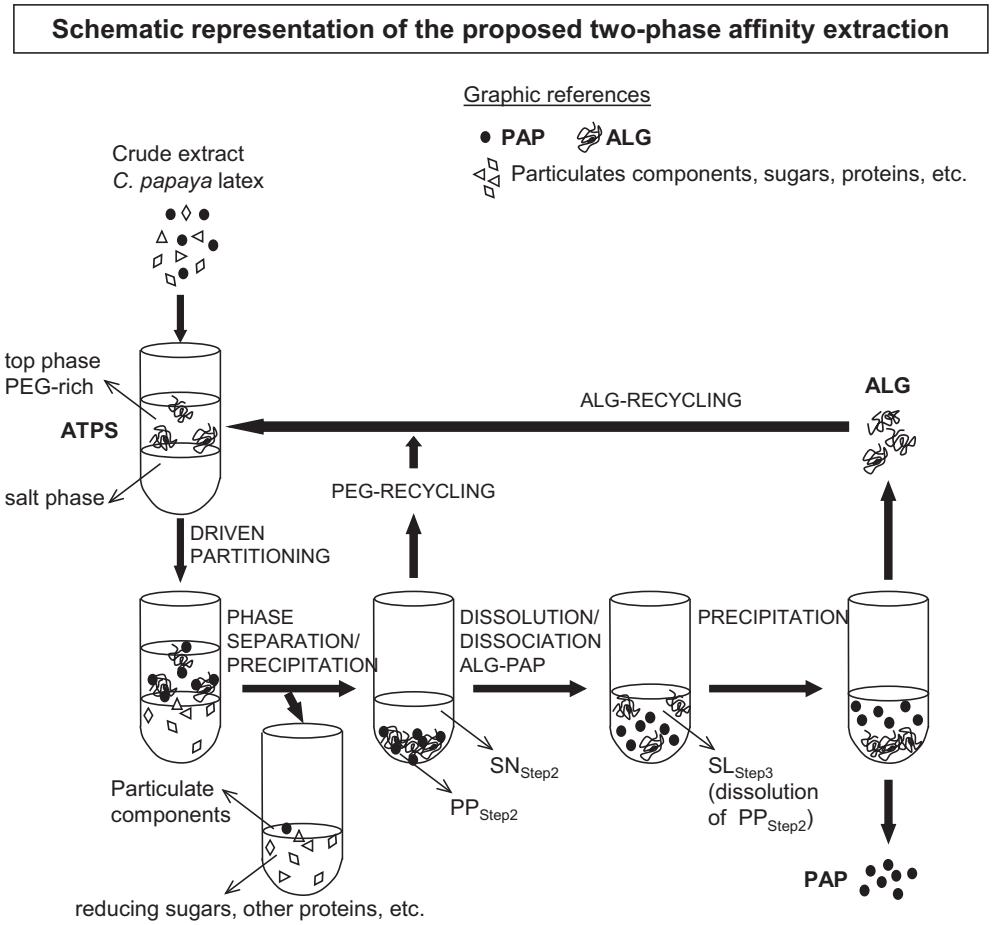

Fig. 7. Schematic representation of the affinity partitioning strategy designed to recover PAP from *C. papaya* latex. Protocol details are indicated in Section 2.2.4.

step, 1 M $CaCl_2$ solution was added to the SL_{Step3} until a final concentration of 100 mM. This procedure is not mandatory since ALG does not interfere with most PAP applications and even acts as a stabilizing agent of the enzyme [43]. The purification indicators obtained are listed in Table 4.

Table 4
Performance of two-phase affinity extraction of PAP from *C. papaya* latex using ALG as affinity macro-ligand.

Extraction step	Total activity (u. Abs./s)	Total protein content (mg)	Specific activity (u. Abs./s mg)	Recovery %	PF
Crude extract	0.375	2.79	0.134	100	1.00
Top $phase_{Step1}$	0.318	1.17	0.271	85	2.01
SN_{Step2}	0.048	0.243	0.201	13	1.50
SL_{Step3}	0.270	0.834	0.323	72	2.41

Composition of PEG8000/NaCit pH 5.20 ATPS is shown in Table 2. C_{ALG} final 0.1% (w/w). Protocol details are indicated in Section 2.2.4. SN_{Step2} is the supernatant of the precipitation with calcium chloride. SL_{Step3} is the solution obtained by dissolving the precipitate of Step 2.

The presence of ALG in the ATPS enhanced PAP recovery at the top phase (step 1) when compared with the recovery in the absence of the ligand (21.9%). However, the PF obtained decreased slightly from 2.48 (without ALG) to 2.01 (with ALG). This suggests that the driving effect of ALG would be taking place not only on PAP but also on other similar proteins present in the latex.

The precipitation and dissolution steps (Step 1 and 2) caused a moderate loss of the target protein (13%) but allowed to obtain a final product of higher purity. The purification factor of 2.41 appears to be meager since the papain represents nearly the 10% of the total protein content in latex [27]. However, by considering that other proteases such as chymopapain and papaya proteinase, which represent the 40% of total protein content in latex, also contribute to the activity measurements against BAPNA, it is reasonable to think that the final product of this extraction contains not only papain but the other cysteine proteases as well. This mixture, commercially known as refined papain, is highly suitable for industrial purposes.

4. Conclusions

The stricter environmental regulations and the higher costs associated to the waste treatment has increased the interest in developing more sustainable industrial processes. Results described in this study demonstrated that papain could be recovered satisfactorily by an affinity two-phase extraction with ATPSs formed by PEG8000 and the biodegradable salt NaCit. The proposed strategy does not require a clarification/filtration step, allows recovering the phase forming polymer PEG to be recycled and yields a final proteolytic product suitable for industrial applications.

An analysis of ALG solutions by different physicochemical approaches allowed us to conclude that the hydrodynamic behavior of this biopolymer was affected by the presence of PAP due to a cooperative interaction protein-polysaccharide enthalpy-entropically driven. Our knowledge of other cysteine proteases such as bromelain and ficin and their structural similarities with papain, allow us to speculate on the possible interaction between ALG and these proteins as well. On this basis, it would expectable that the usefulness of our findings could be extended to the affinity extraction of the mentioned proteins.

Acknowledgements

This research was support by grants from CONICET (PIP0551/12), Argentina, and Agencia Nacional de Promoción Científica y Tecnológica (FONCyT-PICT-2013-1730), Argentina.

Author M. Victoria Rocha gratefully acknowledges the assistance of César Brinatti with ITC measurements.

Author M. Di Giacomo acknowledges Fundación Nuevo Banco de Santa Fe for the research fellowship administered for funding this work.

References

[1] S.E. Barberis, E. Quiroga, C.S. Barcia, C. Liggieri, Effect of laundry detergent formulation on the performance of alkaline phytoproteases, Electron. J. Biotechnol. 16 (2013) 1–8, http://dx.doi.org/10.2225/vol16-issue3-fulltext-1.

[2] Y.Q. Ling, H.L. Nie, S.N. Su, C. Brandford-White, L.M. Zhu, Optimization of affinity partitioning conditions of papain in aqueous two-phase system using response surface methodology, Sep. Purif. Technol. 73 (2010) 343–348, http://dx.doi.org/10.1016/j.seppur.2010.04.020.

[3] M. Lambri, A. Roda, R. Dordoni, M.D. Fumi, Mild process for dehydrated food-grade crude papain powder from papaya fresh pulp: lab-scale and pilot plant experiments, Chem. Eng. Trans. 38 (2014) 7–12, http://dx.doi.org/10.3303/CET1438002.

[4] S. Nitsawang, R. Hatti-Kaul, P. Kanasawud, Purification of papain from *Carica papaya* latex: aqueous two-phase extraction versus two-step salt precipitation, Enzyme Microb. Technol. 39 (2006) 1103–1107, http://dx.doi.org/10.1016/j.enzmictec.2006.02.013.

[5] P.A. Albertsson, Partition of Cell Particles and Macromolecules, Wiley, 1986.

[6] R. Kuboi, W. Wang, I. Komasawa, Effect of contaminating proteins on the separation and purification of papain from papaya latex using aqueous two-phase extraction, Kagaku Kogaku Ronbun. 16 (1990) 772–779, http://dx.doi.org/10.1252/kakoronbunshu.16.772.

[7] M.V. Rocha, B.B. Nerli, Molecular features determining different partitioning patterns of papain and bromelain in aqueous two-phase systems, Int. J. Biol. Macromol. 61 (2013) 204–211, http://dx.doi.org/10.1016/j.ijbiomac.2013.06.055.

[8] L.P. Malpiedi, G.A. Picó, B.B. Nerli, Studies of protein partition in non conventional aqueous two-phase systems as method to purify trypsinogen and alpha-chymotrypsinogen from bovine pancreas, Sep. Purif. Technol. 78 (2011) 91–96, http://dx.doi.org/10.1016/j.seppur.2011.01.026.

[9] G. Tubio, G.A. Picó, B.B. Nerli, Extraction of trypsin from bovine pancreas by applying polyethyleneglycol/sodium citrate aqueous two-phase systems, J. Chromatogr. B 877 (2009) 115–120, http://dx.doi.org/10.1016/j.jchromb.2008.11.016.

[10] S. Teotia, K. Mondal, M.N. Gupta, Integration of affinity precipitation with partitioning methods for bioseparation of chitin binding lectins, Food Bioprod. Process. 84 (2006) 37–43, http://dx.doi.org/10.1205/fbp.05133.

[11] S. Teotia, M.N. Gupta, Reversibly soluble macroaffinity ligand in aqueous two-phase separation of enzymes, J. Chromatogr. A 923 (2001) 275–280, http://dx.doi.org/10.1016/S0021-9673(01)00968-2.

[12] S. Teotia, R. Lata, M.N. Gupta, Free polymeric bioligands in aqueous two-phase affinity extractions of microbial xylanases and pullulanase, Protein Express Purif. 488 (2001) 484–488, http://dx.doi.org/10.1006/prep.2001.1466.

[13] A. Kumar, A. Srivastava, I. Yu, B. Mattiasson, Smart polymers: physical forms and bioengineering applications, Prog. Polym. Sci. 32 (2007) 1205–1237, http://dx.doi.org/10.1016/j.progpolymsci.2007.05.003.

[14] S. Teotia, S.K. Khare, M.N. Gupta, An efficient purification process for sweet potato beta-amylase by affinity precipitation with alginate, Enzyme Microb. Technol. 28 (2001) 792–795, http://dx.doi.org/10.1016/S0141-0229(01)00338-6.

[15] S. Teotia, M.N. Gupta, Purification of phospholipase D by two-phase affinity extraction, J. Chromatogr. A 1025 (2004) 297–301, http://dx.doi.org/10.1016/j.chroma.2003.10.104.

[16] A. Bhattacharyya, S. Dutta, P. De, P. Ray, S. Basu, Removal of mercury (II) from aqueous solution using papain immobilized on alginate bead: optimization of immobilization condition and modeling of removal study, Bioresour. Technol. 101 (2010) 9421–9428, http://dx.doi.org/10.1016/j.biortech.2010.06.126.

[17] F.C. Vasconcellos, G.A.S. Goulart, M.M. Beppu, Production and characterization of chitosan microparticles containing papain for controlled release applications, Powder Technol. 205 (2011) 65–70, http://dx.doi.org/10.1016/j.powtec.2010.08.066.

[18] G. Tubío, L. Pellegrini, B. Nerli, G. Picó, Liquid-liquid equilibria of aqueous two-phase systems containing poly (ethylene glycols) of different molecular weight and sodium citrate, J. Chem. Eng. Data 51 (2006) 209–212, http://dx.doi.org/10.1021/je050332p.

[19] R. Hatti-Kaul, R. Ed, Aqueous Two-Phase Systems: Methods and Protocols, Methods in Biotechnology, vol. 11, Humana Press, New Jersey, 2000.

[20] J.C. Merchuk, B.A. Andrews, J.A. Asenjo, Aqueous two-phase systems for protein separation: studies on phase inversion, J. Chromatogr. B, Biomed. Sci. Appl. 711 (1998) 285–293, http://dx.doi.org/10.1016/S0378-4347(97)00594-X.

[21] M. Azarkan, R. Dibiani, C. Baulard, D. Baeyens-Volant, Effects of mechanical wounding on *Carica papaya* cysteine endopeptidases accumulation and activity, Int. J. Biol. Macromol. 38 (2006) 216–224, http://dx.doi.org/10.1016/j.ijbiomac.2006.02.021.

[22] O. Warburg, W. Christian, Isolation and crystallization of enolase, Biochem. Z 310 (1942) 384–421.

[23] G. Miller, Use of dinitrosalicylic acid reagent for determination of reducing sugar, Anal. Chem. 31 (1959) 426–428, http://dx.doi.org/10.1021/ac60147a030.

[24] M. Dubois, K.A. Gilles, J.K. Hamilton, P.A. Rebers, F. Smith, Colorimetric method for determination of sugars and related substances, Anal. Chem. 28 (1956) 350–356, http://dx.doi.org/10.1021/ac60111a017.

[25] S.E. Harding, The intrinsic viscosity of biological macromolecules. Progress in measurement, interpretation and application to structure in dilute solution, Prog. Biophys. Mol. Biol. 68 (1997) 207–262, http://dx.doi.org/10.1016/S0079-6107(97)00027-8.

[26] A. Sionkowska, Molecular interactions in collagen and chitosan blends, Biomaterials 25 (2004) 795–801, http://dx.doi.org/10.1016/S0142-9612(03)00595-7.

[27] M. Azarkan, A. El Moussaoui, D. Van Wuytswinkel, G. Dehon, Y. Looze, Fractionation and purification of the enzymes stored in the latex of *Carica papaya*, J. Chromatogr., B: Anal. Technol. Biomed. Life Sci. 790 (2003) 229–238, http://dx.doi.org/10.1016/S1570-0232(03)00084-9.

[28] W. Wang, A.A. Ignatius, S.V. Thakkar, Impact of residual impurities and contaminants on protein stability, J. Pharm. Sci. 103 (2014) 1315–1330, http://dx.doi.org/10.1002/jps.23931.

[29] H.C. Sox, Landmark Papers in Internal Medicine: The First 80 Years of Annals of Internal Medicine, first ed., American College of Physicians, 2009.

[30] J. Zeng, R.A. Dunlop, K.J. Rodgers, M.J. Davies, Evidence for inactivation of cysteine proteases by reactive carbonyls via glycation of active site thiols, Biochem. J. 398 (2006) 197–206, http://dx.doi.org/10.1042/BJ20060019.

[31] K. Mondal, P. Mehta, M.N. Gupta, Affinity precipitation of Aspergillus niger pectinase by microwave-treated alginate, Protein Expr. Purif. 33 (2004) 104–109, http://dx.doi.org/10.1016/j.pep.2003.08.013.

[32] S. Teotia, R. Lata, M.N. Gupta, Chitosan as a macroaffinity ligand: purification of chitinases by affinity precipitation and aqueous two-phase extractions, J. Chromatogr. A 1052 (2004) 85–91, http://dx.doi.org/10.1016/j.chroma.2004.08.096.

[33] K. Mondal, M.N. Gupta, The affinity concept in bioseparation: evolving paradigms and expanding range of applications, Biomol. Eng. 23 (2006) 59–76, http://dx.doi.org/10.1016/j.bioeng.2006.01.004.

[34] K. Monkos, Viscosity analysis of the temperature dependence of the solution conformation of ovalbumin, Biophys. Chem. 85 (2000) 7–16, http://dx.doi.org/10.1016/S0301-4622(00)00127-7.

[35] D. Zhong, X. Huang, H. Yang, R. Cheng, New insights into viscosity abnormality of sodium alginate aqueous solution, Carbohydr. Polym. 81 (2010) 948–952, http://dx.doi.org/10.1016/j.carbpol.2010.04.012.

[36] I.M.N. Vold, K.A. Kristiansen, B.E. Christensen, A study of the chain stiffness and extension of alginates, in vitro epimerized alginates, and periodate-oxidized alginates using size-exclusion chromatography combined with light scattering and viscosity detectors, Biomacromolecules 7 (2006) 2136–2146, http://dx.doi.org/10.1021/bm060099n.

[37] J. Yang, S. Chen, Y. Fang, Viscosity study of interactions between sodium alginate and CTAB in dilute solutions at different pH values, Carbohydr. Polym. 75 (2009) 333–337, http://dx.doi.org/10.1016/j.carbpol.2008.07.037.

[38] S. Ghosh, Conformational study of papain in the presence of sodium dodecyl sulfate in aqueous medium, Colloids Surf. B 41 (2005) 209–216, http://dx.doi.org/10.1016/j.colsurfb.2004.12.004.
[39] Y. Zhao, F. Li, M.T. Carvajal, M.T. Harris, Interactions between bovine serum albumin and alginate: an evaluation of alginate as protein carrier, J. Colloid Interface Sci. 332 (2009) 345–353, http://dx.doi.org/10.1016/j.jcis.2008.12.048.
[40] A.M.F. Lima, V. Soldi, R. Borsali, Dynamic light scattering and viscosimetry of aqueous solutions of pectin, sodium alginate and their mixtures: effects of added salt, concentration, counterions, temperature and chelating agent, J. Braz. Chem. Soc. 20 (2009) 1705–1714, http://dx.doi.org/10.1590/S0103-50532009000900020.
[41] C. Tanford, Physical Chemistry of Macromolecules, Wiley, 1961.
[42] D. Guzey, D.J. McClements, Characterization of β-lactoglobulin-chitosan interactions in aqueous solutions: a calorimetry, light scattering, electrophoretic mobility and solubility study, Food Hydrocoll. 20 (2006) 124–131, http://dx.doi.org/10.1016/j.foodhyd.2005.03.009.
[43] M.G. Sankalia, R.C. Mashru, J.M. Sankalia, V.B. Sutariya, Papain entrapment in alginate beads for stability improvement and site-specific delivery: physicochemical characterization and factorial optimization using neural network modeling, AAPS Pharm. Sci. Technol. 6 (2005) E209–E222, http://dx.doi.org/10.1208/pt060231.